

OPEN

# The Effect of Cervical Interbody Cage Morphology, Material Composition, and Substrate Density on Cage Subsidence

Paul B. Suh, MD  
 Christian Puttlitz, PhD  
 Chad Lewis, PhD  
 B. Sonny Bal, MD, MBA, JD, PhD  
 Kirk McGilvray, PhD

From the Orthopaedic Specialists of North Carolina, Raleigh, NC (Dr. Suh); the Orthopaedic Bioengineering Research Laboratory, Department of Mechanical Engineering, and School of Biomedical Engineering, Colorado State University, Fort Collins, CO (Dr. Puttlitz and Dr. McGilvray); Amedica, Salt Lake City, UT (Dr. Lewis and Dr. Bal); and the Department of Orthopaedic Surgery, University of Missouri, Columbia, MO (Dr. Bal).

Correspondence to Dr. McGilvray: [kirk.mcgilvray@gmail.com](mailto:kirk.mcgilvray@gmail.com).

This work was funded by Amedica, Salt Lake City, Utah.

*J Am Acad Orthop Surg* 2016;0:1-9

DOI: 10.5435/JAAOS-D-16-00390

Copyright 2016 by the American Academy of Orthopaedic Surgeons. This is an open-access article distributed under the terms of the Creative Commons Attribution-Non Commercial-No Derivatives License 4.0 (CCBY-NC-ND), where it is permissible to download and share the work provided it is properly cited. The work cannot be changed in any way or used commercially without permission from the journal.

## Abstract

**Background:** Interbody cages used in spinal fusion surgery can subside into the adjacent vertebral bodies after implantation, leading to loss of spinal height, malalignment, and possible radicular symptoms. Several factors may contribute to cage subsidence.

**Methods:** This in vitro investigation examined the possible contribution of substrate density, cage contact area (ie, cage footprint), cage filling, cage end plate surface texture, and cage material composition on the magnitude of subsidence. Commercially available cervical interbody cages of two sizes (16 × 12 mm and 17 × 14 mm) were implanted between foam blocks of two different densities and were cyclically loaded. Cages were made of titanium alloy (Ti<sub>4</sub>Al<sub>6</sub>V), silicon nitride ceramic (Si<sub>3</sub>N<sub>4</sub>), or polyether ether ketone (n = 8 cages of each material type). Additional testing was performed on Si<sub>3</sub>N<sub>4</sub> cages of the smaller size with nontextured surfaces and with filled cores.

**Results:** Subsidence measurements showed that lower foam density had the greatest influence on subsidence, followed by smaller cage footprint. Cage material had no effect on subsidence. In the additional testing of small-footprint Si<sub>3</sub>N<sub>4</sub> cages, the cages in which the core was filled with a load-bearing porous material had less subsidence in lower-density foam than the cages with an empty core had, whereas cage end plate surface texture had no effect on subsidence.

**Conclusion:** Ranking of the relative impact of these factors indicated that substrate density had the greatest contribution to the measured subsidence (approximately 1.7 times and approximately 67 times greater than the contributions of cage footprint area and material, respectively). The contribution of cage footprint area to subsidence was found to be 40 times greater than the contribution of cage material to subsidence.

In cervical spine fusion surgery, vertebral interbody spacers preserve disk height and sagittal alignment, thereby avoiding neural compression and kyphotic collapse.<sup>1</sup> Subsidence refers to an undesirable penetration of the interbody cage into

adjacent vertebral bone, which, when severe enough, can lead to radicular pain and loss of sagittal plane alignment.<sup>2</sup> A clinical study demonstrated >2 mm loss of disk space height in 77% of patients with paired rectangular lumbar fusion cages.<sup>3</sup>

Although several factors have been shown to contribute to subsidence, the interactions between these factors is unclear. In an experimental model using polyurethane foam blocks and an expandable cage design, increases in the angular mismatch between the cage and end plate surfaces led to progressively greater subsidence.<sup>4</sup> In a study of lateral lumbar interbody fusion, more subsidence occurred when narrower rather than wider cages were used, although clinical outcomes were similar between the study groups.<sup>5</sup> A biomechanical study of cadaver cervical spines showed that end plate destruction resulting from surgical preparation reduces the ability of the spine to withstand compressive loads, thereby contributing to the risk of subsidence.<sup>6</sup> Cage geometries that have a larger surface contact area with bone have also been shown to result in less subsidence.<sup>7</sup> Although each of these studies identified one or two factors that influenced cage subsidence, the relative contribution of multiple combined factors to subsidence remains unknown.

Vertebral interbody cages are often made of polyether ether ketone (PEEK) because this material is inexpensive, is radiolucent, and has a modulus of elasticity that approximates that of cortical bone.<sup>8</sup> In contrast to roughened titanium alloy surfaces that promote osteogenesis when implanted in living bone, PEEK surfaces result in the development of fibrous tissue.<sup>9</sup> Therefore, cages made of PEEK are usually packed with bone graft to achieve

spinal fusion. Alternatively, cages may be made of porous materials that support bony healing into the cage itself, such as metal alloys and/or ceramic materials.<sup>10-14</sup>

The purpose of this study was to investigate the contribution of cage material composition, substrate density, cage footprint size, cage surface texture, and cage filling to the degree of subsidence. The relative effect of these factors was ranked to provide the surgeon with a strategy to minimize subsidence.

## Methods

### Testing Substrate

Closed-cell, rigid polyurethane foam (Sawbones; Pacific Research Laboratory) was chosen in two densities to model two discrete scenarios of bone quality. The lower-density foam had a density of 160.19 kg/m<sup>3</sup> and a compressive modulus of 58 MPa, whereas the higher-density foam had a density of 320.37 kg/m<sup>3</sup> and a compressive modulus of 210 MPa. The higher-density foam was intended to model removal of the cartilaginous end plate with complete preservation of the cortical end plate. The lower-density foam was intended to model total removal of the cortical end plate with only cancellous bone remaining. Partial removal of the cortical end plate was not investigated in this study. Test substrates of each density (40.5-mm thickness × 50.8-mm diameter) were prepared from the same manufacturing lot (to reduce

variability) with the use of a 2-inch diameter circular saw.

### Interbody Cages

Commercially available cervical interbody cages of open-core design (Valeo C; Amedica) were tested using three material compositions: Si<sub>3</sub>N<sub>4</sub>, Ti<sub>4</sub>Al<sub>6</sub>V, and PEEK, with eight cages of each material type (Figure 1). These materials have elastic moduli of 296 GPa, 110 GPa, and 4 GPa, respectively.<sup>11</sup> Each cage material was tested in two sizes: 16 × 12 mm, with a footprint area of 103.2 mm<sup>2</sup>, and 17 × 14 mm, with a footprint area of 125.5 mm<sup>2</sup>. The footprint area does not include the cross-sectional area of the graft window. All cages were 10-mm thick and had a 0° lordosis angle. In this portion of the study, the central cavity, designed to hold bone graft, was left unfilled during testing. All of these cages had the same gross morphology of the end plate, with a spiked surface designed to improve mechanical fit. The end plates of the Si<sub>3</sub>N<sub>4</sub> cages also included laser texturing (with a texture depth of approximately 50 to 150 μm) (Figure 1).

To evaluate the effect of cage end plate texture and the filling of the central cavity with a porous material (analogous to bone graft), two additional cage types were investigated. Specifically, two small-footprint Si<sub>3</sub>N<sub>4</sub> cage types with smooth, non-textured end plates were tested. In one group (n = 8), the central cavity was left empty. The cages in the other group (n = 8) were

Dr. Suh or an immediate family member has received royalties from Zimmer Biomet, is a member of a speakers' bureau or has made paid presentations on behalf of Eli Lilly, and serves as a paid consultant to or is an employee of Amedica and Zimmer Biomet. Dr. Puttlitz or an immediate family member serves as a paid consultant to or is an employee of Medtronic Sofamor Danek and has received research or institutional support from Medtronic, the National Institutes of Health (the National Institute of Arthritis and Musculoskeletal and Skin Diseases and the Eunice Kennedy Shriver National Institute of Child Health and Human Development), and Stryker. Dr. Lewis or an immediate family member is an employee of Amedica and Elevate Medical. Dr. Bal or an immediate family member serves as a paid consultant to or is an employee of Amedica, ConforMIS, and MicroPort. Dr. McGilvray or an immediate family member has received research or institutional support from DePuy Synthes, Johnson & Johnson, Medtronic Sofamor Danek, the National Institutes of Health (the National Institute of Arthritis and Musculoskeletal and Skin Diseases and the Eunice Kennedy Shriver National Institute of Child Health and Human Development), Orthofix, and Stryker.

manufactured with a composite design in which the central cavity was filled with porous  $\text{Si}_3\text{N}_4$  (Figure 1).

### Cyclic Loading

The experimental constructs, each consisting of a cage between foam blocks, were axially loaded in a servohydraulic material-testing machine (MTS Systems) with custom-made fixtures to measure subsidence (Figure 2). The experimental apparatus conforms to ASTM standard F2267-04, which is used to assess subsidence risk.<sup>15</sup> To ensure proper alignment of each cage within the testing fixture, a template was used to mark the center of the testing substrates, and the graft window of each cage was centered on the substrates. An alignment jig was used to ensure that the top and bottom fixtures were coaxial before testing (thereby eliminating off-center loading). Cyclic compression between 50 and 250 N (in a sinusoidal wave form) was applied at a rate of 1 Hz under force control feedback. Compression of 50 N corresponds to the load of the average human head on the cervical spine.<sup>16</sup> Because the intent was to examine implant subsidence under cyclic loading, a maximum limit of 250 N was selected to allow a factor of safety with respect to the published failure loads of vertebral body end plates (published failure loads of the implant–end plate interface range from 754 to 2,238 N).<sup>16</sup>

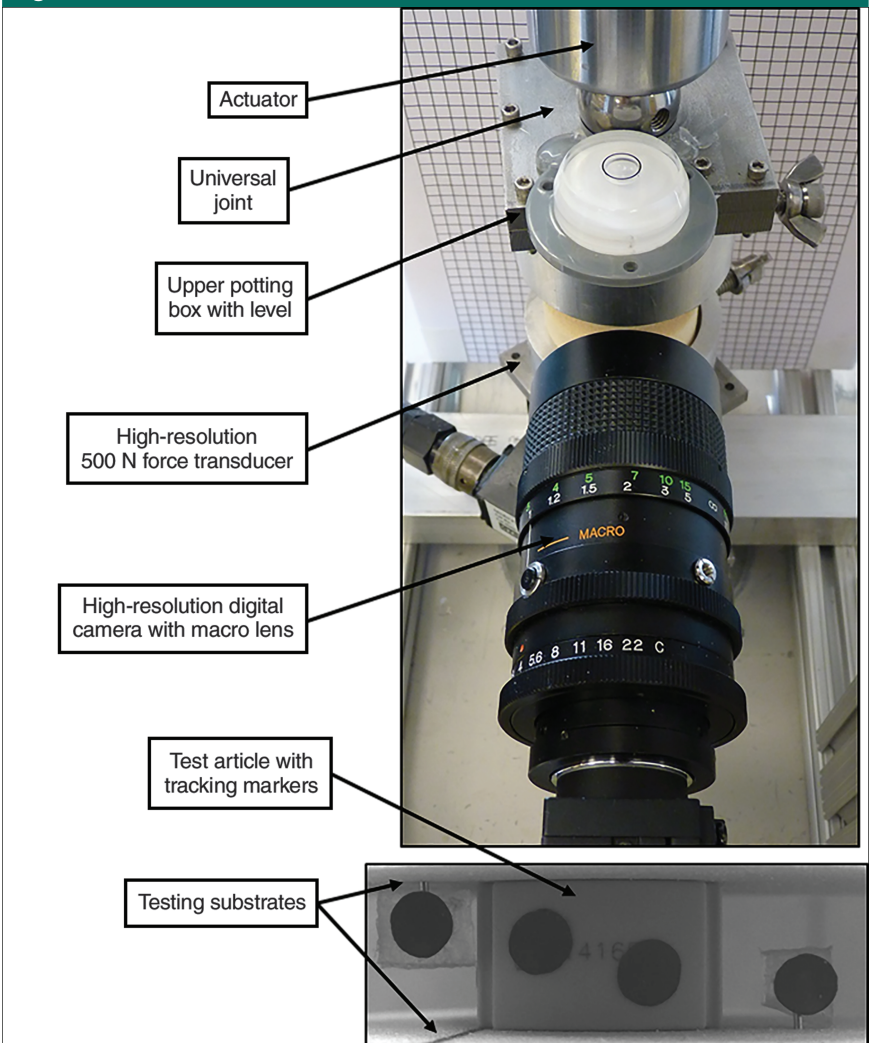
Two tracking markers were fixed to each cage with cyanoacrylate, and one tracking marker was rigidly fixed to each of the adjacent foam blocks. Subsidence was detected with a high-resolution digital camera (Grasshopper 3; Point Grey Research) and an attached macro lens (50 mm/F1.8, No. 86574; Edmund Optics), producing an effective pixel resolution of 5  $\mu\text{m}$ . Digital image correlation (DIC) was used to quantify

**Figure 1**



Illustration depicting the cage types used in the study. The small cages measured 16 × 12 mm; the large cages measured 17 × 14 mm. PEEK = polyether ether ketone

**Figure 2**



Photographs depicting the custom-made testing fixture and the servohydraulic material-testing machine used for cyclic and quasi-static subsidence testing.



subsidence of the cage into the foam blocks after 1 cycle, 500 cycles, 1,000 cycles, 2,000 cycles, and 3,600 cycles. The DIC system demonstrated accuracy to within two pixels with a standard deviation on repeated measurement of <3%. Load and displacement data (ie, DIC images of subsidence) were recorded throughout each cycle of interest at 100 Hz. The maximum number of test cycles was limited to 3,600 because pilot data previously showed that the percentage increase in subsidence beyond 3,600 cycles was negligible (ie, <10% increase in subsidence up to 10,000 cycles). In findings consistent with our observations, other investigators reported that most subsidence occurred during the first 500 cycles of loading.<sup>16</sup>

The DIC data were analyzed with the use of custom software code (MATLAB release R2014a; MathWorks). The geometric centers of the tracking markers were calculated in two-dimensional space, and subsidence was expressed as the mean cage displacement, in micrometers, into the adjacent foam at the highest load for each cycle of interest. Specifically, the distance between the tracking markers on the cage and those on the top and bottom substrates were calculated and averaged. The baseline subsidence value was calculated at the lowest load (ie, 50 N) during the first cycle.

### Ramp-to-Failure Testing

Ramp-to-failure testing was performed to assess the stiffness and yield point of the foam-cage-foam constructs, in accordance with the ASTM F2267-04 standard for cervical devices. This testing was performed to understand how the factors contribute to catastrophic failure. Compressive loads were applied quasi-statically at a rate of 0.1 mm/s to the foam-cage-foam constructs. The load and displacement

data were recorded at 100 Hz; output parameters of the ramp-to-failure testing included yield load and construct stiffness (in newtons per millimeter). Yield load was defined as the applied force required to cause a permanent deformation equal to the offset displacement (ie, 1-mm offset, according to the ASTM F2267-04 standard for cervical devices). The quasi-static system stiffness was the slope of the initial linear portion of the load-displacement curve. Stiffness was calculated between 200 and 250 N of compressive loading for all foam-cage-foam constructs.

### Statistical Analyses

Power calculations using pilot data and R statistical software<sup>17</sup> demonstrated that a minimum of eight samples per test group was required to achieve statistical significance (inputs and outputs were as follows: power = 0.8, delta = 0.21, standard deviation [SD] = 0.11,  $P = 0.01$ , type = “two-sample,” alternative = “two-sided,”  $n = 8.0$ ).

To examine the effects and interactions of foam density (high versus low), cage footprint area (small versus large), and cage material ( $\text{Si}_3\text{N}_4$ ,  $\text{Ti}_4\text{Al}_6\text{V}$ , or PEEK) on subsidence (measured at selected cycles), a general linear model was used to analyze the multiple effects. Similarly, the effects and interactions of cage design (ie, presence or absence of a textured contact surface, open or filled central cavity) and foam density were also assessed using a general linear model. To determine the relative contribution of each effect (foam density, cage footprint area, and material) on subsidence after 3,600 cycles, a model comparison approach was used.<sup>18</sup> All comparisons were determined using Tukey post hoc adjusted least squares means to control type I error rate. Statistical tests were performed with Minitab 15 statistical software (Minitab) with  $\alpha = 0.05$ .

## Results

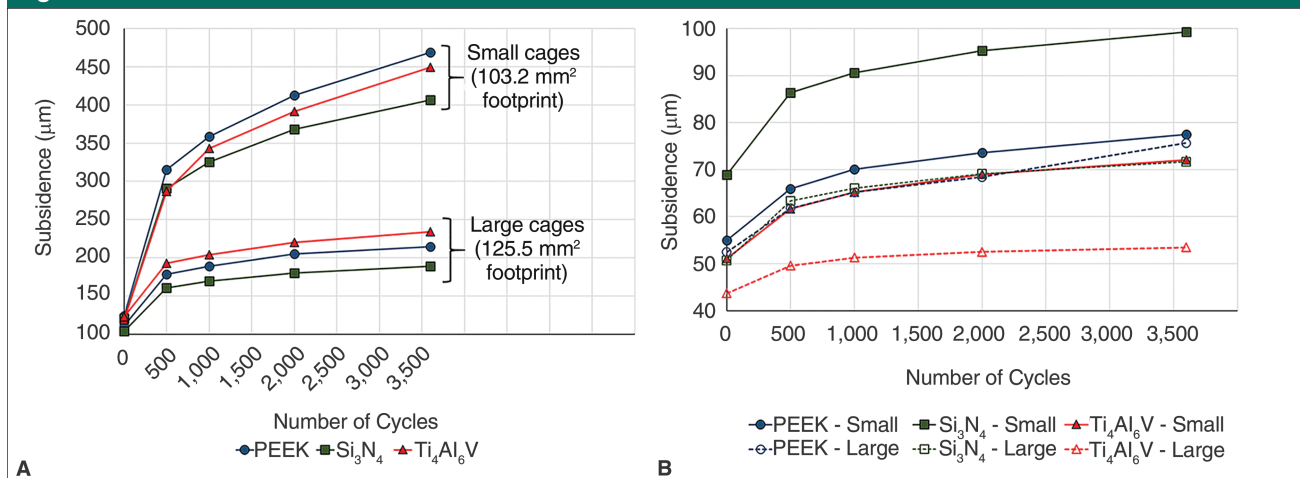
All biomechanical tests were run to completion with no cage damage or experimental complications. Statistical analyses were performed after 3,600 cycles. All data passed normality and equal variance tests.

### Effects of Foam Density, Cage Footprint, and Cage Material on Subsidence

Subsidence increased as the number of cycles increased across all test groups (Figure 3). Foam density and cage footprint area had significant effects on subsidence after 3,600 cycles (both  $P < 0.01$ ), whereas cage material composition did not have a significant effect ( $P = 0.20$ ). Lower-density foam was associated with significantly greater subsidence compared with higher-density foam ( $P < 0.01$ ) (Figures 3 and 4). In lower-density foam, the small-footprint cages had significantly greater subsidence (approximately 5.3 times greater) than the large-footprint cages had ( $P < 0.01$ ) (Figures 3 and 4). Subsidence magnitudes were notably reduced when higher-density foam was used, which substantially diminished the effects of the footprint area on subsidence ( $P = 0.49$ ) (Table 1). Interestingly, subsidence was significantly greater for  $\text{Ti}_4\text{Al}_6\text{V}$  and PEEK cages compared with  $\text{Si}_3\text{N}_4$  cages when tested with lower-density foam (both  $P < 0.05$ , small-footprint cages:  $\text{Si}_3\text{N}_4$ ,  $406 \pm 91 \mu\text{m}$ ;  $\text{Ti}_4\text{Al}_6\text{V}$ ,  $449 \pm 61 \mu\text{m}$ ; PEEK,  $468 \pm 36 \mu\text{m}$ ; large-footprint cages:  $\text{Si}_3\text{N}_4$ ,  $189 \pm 22 \mu\text{m}$ ;  $\text{Ti}_4\text{Al}_6\text{V}$ ,  $233 \pm 38 \mu\text{m}$ ; PEEK,  $214 \pm 37 \mu\text{m}$ ) (Figure 4). Testing with higher-density foam revealed no significant differences between the cage materials (all  $P \geq 0.57$ ; small-footprint cages:  $\text{Si}_3\text{N}_4$ ,  $99 \pm 15 \mu\text{m}$ ;  $\text{Ti}_4\text{Al}_6\text{V}$ ,  $72 \pm 18 \mu\text{m}$ ; PEEK,  $77 \pm 15 \mu\text{m}$ ; large-footprint cages:  $\text{Si}_3\text{N}_4$ ,  $71 \pm 12 \mu\text{m}$ ;  $\text{Ti}_4\text{Al}_6\text{V}$ ,



Figure 3



Graphs depicting the mean subsidence per number of loading cycles for each cage size and cage material for lower-density foam (A) and higher-density foam (B). The lower-density foam (A) and smaller cage size were associated with more subsidence. With the higher-density foam (B), differences in subsidence between the two implant sizes were reduced. PEEK = polyether ether ketone

Table 1

Subsidence After Cyclic Loading According to Cage Size, Cage Material, and Substrate

No. of Cycles	Cage Size (mm)	Subsidence ( $\mu\text{m}$ ) <sup>a</sup>					
		Lower-Density Foam Substrate			Higher-Density Foam Substrate		
		Si <sub>3</sub> N <sub>4</sub> Cage	Ti <sub>4</sub> Al <sub>6</sub> V Cage	PEEK Cage	Si <sub>3</sub> N <sub>4</sub> Cage	Ti <sub>4</sub> Al <sub>6</sub> V Cage	PEEK Cage
1	16 × 12	120 ± 18	118 ± 9	123 ± 7	68 ± 10	51 ± 11	55 ± 4
	17 × 14	103 ± 7	122 ± 28	111 ± 8	50 ± 7	43 ± 4	52 ± 4
500	16 × 12	291 ± 61	286 ± 34	315 ± 20	86 ± 12	61 ± 13	65 ± 12
	17 × 14	160 ± 13	192 ± 33	178 ± 24	63 ± 11	49 ± 5	61 ± 7
1,000	16 × 12	325 ± 65	342 ± 36	358 ± 25	90 ± 13	65 ± 14	70 ± 12
	17 × 14	169 ± 16	204 ± 34	188 ± 30	66 ± 12	51 ± 5	65 ± 8
2,000	16 × 12	368 ± 78	391 ± 52	412 ± 28	95 ± 14	69 ± 16	73 ± 13
	17 × 14	180 ± 19	219 ± 36	204 ± 33	69 ± 11	52 ± 5	68 ± 9
3,600	16 × 12	406 ± 91	449 ± 61	468 ± 36	99 ± 15	72 ± 18	77 ± 15
	17 × 14	189 ± 22	233 ± 38	214 ± 37	71 ± 12	53 ± 6	75 ± 15

PEEK = polyether ether ketone

<sup>a</sup> Subsidence is given as mean ± standard deviation.

53 ± 6  $\mu\text{m}$ ; PEEK, 75 ± 15  $\mu\text{m}$ ) (Table 1 and Figure 4).

### Effects of End Plate Surface Texture and Core Filling on Subsidence

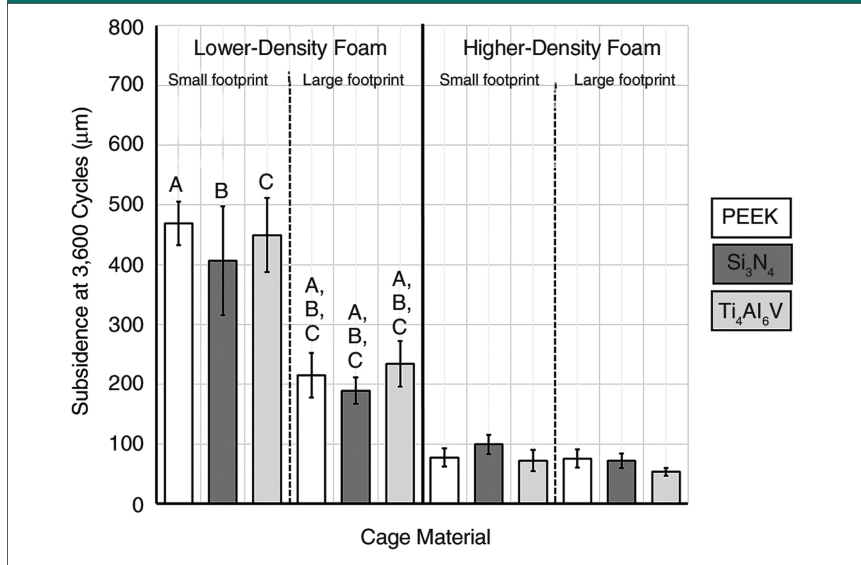
To test the effects of end plate surface texture and filling of the central cavity with a load-bearing porous mate-

rial, two additional variations of the small-footprint Si<sub>3</sub>N<sub>4</sub> cage were tested for subsidence. One variation had a nontextured end plate surface with an empty cavity. The other variation was identical to the original small-footprint Si<sub>3</sub>N<sub>4</sub> cage except that the central cavity was filled with porous Si<sub>3</sub>N<sub>4</sub>. Data were compared with those obtained previously for

the small-footprint Si<sub>3</sub>N<sub>4</sub> cages (Table 2).

At 3,600 cycles, cages with textured end plates had less subsidence than nontextured cages had in testing with lower-density foam, but the difference was not statistically significant (406 ± 91  $\mu\text{m}$  versus 513 ± 2  $\mu\text{m}$ ;  $P = 0.06$ ). End plate texture also did not significantly affect subsidence in

**Figure 4**



and those with nonfilled cores was not significant ( $P = 0.99$ ; filled,  $93 \pm 8 \mu\text{m}$ ; nonfilled textured,  $99 \pm 15 \mu\text{m}$ ; nonfilled nontextured,  $78 \pm 0 \mu\text{m}$ ).

### Relative Contribution of Foam Density, Footprint Area, and Material to Subsidence

Using the model comparison approach, the proportional reduction in error was found to be 0.78 for foam density, 0.46 for cage footprint area, and 0.01 for cage material. Thus, foam density had the greatest contribution to the measured subsidence (approximately 1.7 times and approximately 67 times greater than the contributions of footprint area and material, respectively). The relative contribution of cage contact area to subsidence was found to be 40 times greater than the contributions of variations in material.

Bar graph depicting subsidence at 3,600 cycles of loading with 50 to 250 N of compression. Data are means; error bars indicate standard deviation. Paired letters A, B, and C indicate statistically significant differences ( $P < 0.01$ ). Statistically significant differences in subsidence were also observed between all lower-density foam samples and their corresponding higher-density foam samples for both cage sizes and all cage materials ( $P \leq 0.01$ ). PEEK = polyether ether ketone

**Table 2**

**Subsidence of Small-footprint Si<sub>3</sub>N<sub>4</sub> Cages After Cyclic Loading According to Cage End Plate Surface Texture and Cage Filling**

No. of Cycles	Subsidence ( $\mu\text{m}$ ) <sup>a</sup>					
	Lower-Density Foam Substrate			Higher-Density Foam Substrate		
	Regular Cage <sup>b</sup>	Nontextured Cage	Filled Cage	Regular Cage <sup>b</sup>	Nontextured Cage	Filled Cage
1	120 ± 18	133 ± 2	137 ± 8	68 ± 10	52 ± 18	61 ± 1
500	291 ± 61	365 ± 3	185 ± 24	86 ± 12	74 ± 0	83 ± 5
1,000	325 ± 63	416 ± 8	194 ± 26	90 ± 11	75 ± 1	87 ± 7
2,000	368 ± 78	470 ± 9	203 ± 29	95 ± 14	77 ± 1	89 ± 9
3,600	406 ± 91	513 ± 2	212 ± 31	99 ± 15	78 ± 0	93 ± 8

<sup>a</sup> Subsidence is given as mean ± standard deviation.

<sup>b</sup> Regular indicates the standard Si<sub>3</sub>N<sub>4</sub> cage type (textured end plate surface and no central cavity filling).

### Construct Stiffness and Offset Yield Load

No significant differences in the foam-cage-foam construct stiffness were found between cage materials ( $P = 0.946$ ; PEEK,  $642.1 \pm 343.3 \text{ N/mm}$ ; Si<sub>3</sub>N<sub>4</sub>,  $647.0 \pm 375.0 \text{ N/mm}$ ; Ti<sub>4</sub>Al<sub>6</sub>V,  $660.0 \pm 390.0 \text{ N/mm}$ ). Although the larger footprint area had greater stiffness, the footprint area was not found to have a significant effect on construct stiffness ( $P = 0.122$ ; large footprint,  $685.9 \pm 344.1 \text{ N/mm}$ ; small footprint,  $613.3 \pm 380.3 \text{ N/mm}$ ). Foam density had the greatest effect on construct stiffness; specifically, the higher-density foam constructs had, on average, three times more stiffness than the lower-density foam constructs had ( $P < 0.001$ ;  $980.8 \pm 174.1 \text{ N/mm}$  and  $318.5 \pm 57.6 \text{ N/mm}$ , respectively). The offset yield was significantly greater in higher-density foam than in lower-density foam when data were averaged

testing with higher-density foam ( $P = 0.99$ ;  $99 \pm 15 \mu\text{m}$  with texture versus  $78 \pm 0 \mu\text{m}$  without texture). A notable reduction in subsidence was observed in cages in which the core was filled with load-bearing porous Si<sub>3</sub>N<sub>4</sub> compared with cages

with an empty core (with or without textured end plates) in lower-density foam ( $P < 0.01$ ; filled,  $212 \pm 31 \mu\text{m}$ ; nonfilled textured,  $406 \pm 91 \mu\text{m}$ ; nonfilled nontextured,  $513 \pm 2 \mu\text{m}$ ). In higher-density foam, the difference between cages with filled cores

Table 3

Ramp-to-Failure Data<sup>a</sup>

Cage Material	Cage Size (mm)	Lower-Density Foam Substrate		Higher-Density Foam Substrate	
		Stiffness (N/mm)	Offset Yield (N)	Stiffness (N/mm)	Offset Yield (N)
Si <sub>3</sub> N <sub>4</sub>	16 × 12	259.8 ± 26.8	-368.7 ± 9.5	995.9 ± 261.6	-1,469.8 ± 5.9
	17 × 14	366.5 ± 7.4	-432.8 ± 7.8	964.9 ± 159.6	-1,880.1 ± 17.2
Ti <sub>4</sub> Al <sub>6</sub> V	16 × 12	259.8 ± 25.4	-368.2 ± 7.7	913.5 ± 194.8	-1,472.9 ± 19.9
	17 × 14	371.16 ± 4.5	-426.6 ± 18.8	1,095.7 ± 230.1	-1,785.6 ± 25.9
PEEK	16 × 12	274.5 ± 14.0	-355.6 ± 11.5	976.5 ± 146.8	-1,416.9 ± 27.0
	17 × 14	379.3 ± 13.0	-417.7 ± 19.6	938.1 ± 146.1	-1,795.3 ± 14.2

PEEK = polyether ether ketone

<sup>a</sup> All data are given as mean ± standard deviation.

across all other variables ( $P < 0.01$ ;  $-1,636 \pm 193$  N versus  $-395 \pm 34$  N). In addition, the offset yield was greater for the large-footprint area than for the small-footprint area ( $P < 0.01$ ;  $-1,123 \pm 718$  N versus  $-909 \pm 561$  N). Ramp-to-failure testing highlighted that the denser substrate provided a stiffer construct and higher yield point (Table 3). Other factors, including cage material and cage size, did not show significant differences in construct stiffness and yield point.

## Discussion

This biomechanical investigation was designed to simulate cyclic, axial loading in the cervical spine after single-level fusion with a spacer device. The loads applied were similar to physiologic conditions in the human cervical spine. Our methods allowed the detection of subsidence at the 5- $\mu$ m level; thus, the experimental setup allowed increased fidelity compared with that of a digital radiograph.<sup>19</sup> This consistent and reproducible model, coupled with the high measurement sensitivity, yielded data that allowed determination of the relative impact of different factors on cage subsidence. The results demonstrated that lower substrate density was associated

with higher subsidence. To a lesser degree, a smaller cage footprint resulted in more subsidence. Also, filling the cage with structural material reduced subsidence in testing with a lower substrate density. Cage material and surface texture had no statistically significant effect on subsidence.

Our findings corroborate those of previous investigations. In a study of cadaver specimens, for example, surgical burring of the cortical end plate led to increased subsidence, as did risk factors for osteoporosis, such as female sex and increasing patient age.<sup>6</sup> Finite element analyses have shown that preservation of the structural integrity of the vertebral end plate protects against subsidence, particularly in the cortical periphery, as does packing of the cage cavity with graft material.<sup>20</sup> Other investigators have found that the material properties of the end plate, modeled as different foam densities in our study, are more important determinants of subsidence than the cage material itself is.<sup>21</sup>

In our study, the large-footprint cages had less subsidence than the small-footprint cages had, suggesting that the area of contact between cage and bone is relevant. Other authors have reported that cages that match the vertebral end plate morphology

result in less subsidence-related neck pain after single-level cervical fusion than other cages do.<sup>22</sup> Biomechanical investigations have also shown that larger-diameter spinal cages can withstand greater loads, with a lower risk to failure, compared with smaller, comparable constructs.<sup>23</sup> In 100 consecutive patients who underwent cervical discectomy and interbody fusion, when subsidence was defined as  $>2$  mm reduction in segmental height, investigators reported that the ratio of the spacer surface area to the end plate surface area was substantially smaller in implants with subsidence than in implants without subsidence.<sup>24</sup>

Other authors have suggested that filling the cage cavity with densely packed bone graft increases the surface area and provides structural support against the vertebral end plate, thereby decreasing the risk of subsidence.<sup>20</sup> When identical interbody cages were tested in a biomechanical model similar to the one used in our study, the cages filled with corticocancellous bone graft had substantially less subsidence than empty cages had at 20,000 cycles of load testing. When subsidence was compared among cervical fusions in which a fibular allograft, a titanium mesh cage packed with cancellous bone chips, or a trabecular metal cage was used



as the interpositional structure, the latter two constructs subsided less, which the authors of the study attributed to a larger cage surface contact area.<sup>16</sup>

Our results show that foam density had the most influence on subsidence risk, suggesting that the bone quality of the vertebral end plate and/or the vertebral body is important in predicting subsidence. Destructive compression testing and finite element analyses have shown that load to failure is associated with bone mineral density but not with end plate thickness.<sup>25</sup> Load to failure decreases with progressive removal of the end plate, such that specimens with an intact end plate failed at substantially higher loads than those with no end plate did.<sup>25</sup> Three-dimensional experimental models of the cervical spine have suggested a high correlation between decreasing bone mineral density and increasing amounts of subsidence.<sup>26</sup>

Interbody cages made of PEEK are well accepted by clinicians because, at least in theory, PEEK may produce lower contact stresses, resulting in less subsidence.<sup>26</sup> The Young modulus of PEEK (4 GPa) is closer to that of cancellous bone (100 MPa) compared with the other materials examined and is much lower than that of Ti<sub>4</sub>Al<sub>6</sub>V.<sup>26</sup> Although these numbers suggest that a stiffer material should subside more, several studies have shown instead that the bone quality (ie, degree of vertebral body osteoporosis) and end plate integrity are the dispositive factors affecting subsidence risk.<sup>27</sup> Our data show that cage material composition did not affect subsidence, even though the materials tested had a 100-fold difference in the modulus of elasticity.

The present study has limitations. The foam used to mimic vertebral segments is homogenous and isotropic and cannot completely model the mechanical behavior of living

bone, which is anisotropic, with a cortical end plate and cancellous core. Also, only axial loads were applied in our study, while in vivo cervical loads reflect complex shear and rotational vectors in addition to axial forces. We modeled loading in both routine physiologic cyclic loads as well as loads resulting in catastrophic failure. Our model was purely biomechanical and did not consider biologic responses to cages, which may also contribute to subsidence. The model was limited to only two densities of foam and two implant sizes; therefore, caution should be used when interpreting these results across the clinically relevant spectrum of bone qualities and implant sizes.

Additional limitations of our study relate to the fact that the cages were left empty during mechanical testing instead of being filled manually with bone graft or related material, as is done clinically. We chose to test the cages in their manufactured state, that is, with empty cores, to maximize the effect of the material modulus on cage subsidence and to avoid the potential variation in cage density that manual packing of bone graft might induce. Also, the Si<sub>3</sub>N<sub>4</sub> cages that were manufactured with a porous Si<sub>3</sub>N<sub>4</sub> core offered a clean comparison to the identically designed cages made of the same size and material but with an empty core. These composite Si<sub>3</sub>N<sub>4</sub> cages, which require no bone graft, are used clinically in Europe but are not available in the United States.

## Conclusion

Prior studies of cage subsidence have investigated one or two factors leading to subsidence. Our study investigated five factors in a cohesive and systematic fashion to determine the relative contribution of each factor to cage subsidence. The ranking of these

factors can help surgeons develop a more precise strategy to avoid cage subsidence.

With the limitations of the study in mind, our results allow the following meaningful conclusions. First, although end plate preparation for interbody fusion must include removal of the cartilaginous end plate to facilitate fusion, our data suggest that the surgeon should preserve the cortical end plate and avoid perforating the cancellous bone to reduce the risk of subsidence. The peripheral rim of the end plate has thicker cortical bone and may need to be burred to flatten the end plate surface to match the cage surface. Second, in the present study, the larger cage size resulted in less subsidence in the less dense substrate. Therefore, the use of larger cages in vivo may result in much less subsidence because they are positioned on stronger bone in the periphery of the end plate, independent of cage size. We observed that filling the cage with robust structural material reduced subsidence in the less dense substrate. Furthermore, although cage footprint geometry and texture may contribute to initial cage stability, these variables do not appear to influence cage subsidence. Finally, the intrinsic stiffness of the cage material (PEEK, Ti<sub>4</sub>Al<sub>6</sub>V, or Si<sub>3</sub>N<sub>4</sub>) had no effect on subsidence in our study.

## References

*Evidence-based Medicine:* Levels of evidence are described in the table of contents. In this article, reference 22 is a level I study. References 5, 9, 14, and 23 are level II studies. References 2, 3, 10, 11, 19, 24, and 25 are level III studies. References 4, 6, 7, 12, 16, 20, 21, 26, and 27 are level IV studies. References 1, 8, 13, 15, 17, and 18 are level V expert opinion.

References printed in **bold type** are those published within the past 5 years.

1. Weiner BK, Fraser RD: Spine update: Lumbar interbody cages [published correction appears in *Spine (Phila Pa 1976)* 1998;23(12):1428]. *Spine (Phila Pa 1976)* 1998;23(5):634-640.
2. Lee YS, Kim YB, Park SW: Risk factors for postoperative subsidence of single-level anterior cervical discectomy and fusion: The significance of the preoperative cervical alignment. *Spine (Phila Pa 1976)* 2014;39(16):1280-1287.
3. Choi JY, Sung KH: Subsidence after anterior lumbar interbody fusion using paired stand-alone rectangular cages. *Eur Spine J* 2006;15(1):16-22.
4. Mohammad-Shahi MH, Nikolaou VS, Giannitsios D, Ouellet J, Jarzem PF: The effect of angular mismatch between vertebral endplate and vertebral body replacement endplate on implant subsidence. *J Spinal Disord Tech* 2013;26(5):268-273.
5. Marchi L, Abdala N, Oliveira L, Amaral R, Coutinho E, Pimenta L: Radiographic and clinical evaluation of cage subsidence after stand-alone lateral interbody fusion. *J Neurosurg Spine* 2013;19(1):110-118.
6. Truumees E, Demetropoulos CK, Yang KH, Herkowitz HN: Failure of human cervical endplates: A cadaveric experimental model. *Spine (Phila Pa 1976)* 2003;28(19):2204-2208.
7. Tan JS, Bailey CS, Dvorak MF, Fisher CG, Oxland TR: Interbody device shape and size are important to strengthen the vertebra-implant interface. *Spine (Phila Pa 1976)* 2005;30(6):638-644.
8. Kurtz SM, Devine JN: PEEK biomaterials in trauma, orthopedic, and spinal implants. *Biomaterials* 2007;28(32):4845-4869.
9. Olivares-Navarrete R, Hyzy SL, Slosar PJ, Schneider JM, Schwartz Z, Boyan BD: Implant materials generate different peri-implant inflammatory factors: Poly-ether-ether-ketone promotes fibrosis and microtextured titanium promotes osteogenic factors. *Spine (Phila Pa 1976)* 2015;40(6):399-404.
10. Bock RM, McEntire BJ, Bal BS, Rahaman MN, Boffelli M, Pezzotti G: Surface modulation of silicon nitride ceramics for orthopaedic applications. *Acta Biomater* 2015;26:318-330.
11. McEntire BJ, Enomoto Y, Zhu W, Boffelli M, Marin E, Pezzotti G: Surface toughness of silicon nitride bioceramics: II. Comparison with commercial oxide materials. *J Mech Behav Biomed Mater* 2016;54:346-359.
12. Pezzotti G, Enomoto Y, Zhu W, Boffelli M, Marin E, McEntire BJ: Surface toughness of silicon nitride bioceramics: I. Raman spectroscopy-assisted micromechanics. *J Mech Behav Biomed Mater* 2016;54:328-345.
13. Bal BS, Rahaman MN: Orthopedic applications of silicon nitride ceramics. *Acta Biomater* 2012;8(8):2889-2898.
14. Schmieder K, Wolzik-Grossmann M, Pechlivanis I, Engelhardt M, Scholz M, Harders A: Subsidence of the wing titanium cage after anterior cervical interbody fusion: 2-year follow-up study. *J Neurosurg Spine* 2006;4(6):447-453.
15. Imwinkelried T: Mechanical properties of open-pore titanium foam. *J Biomed Mater Res A* 2007;81(4):964-970.
16. Ordway NR, Rim BC, Tan R, Hickman R, Fayyazi AH: Anterior cervical interbody constructs: Effect of a repetitive compressive force on the endplate. *J Orthop Res* 2012;30(4):587-592.
17. The R Foundation: The R Project for Statistical Computing. <http://www.r-project.org/>. Accessed November 21, 2016.
18. Judd CM, McClelland GH, Ryan CS: *Data Analysis: A Model Comparison Approach*, ed 2. New York, NY, Routledge, 2009.
19. Bansal GJ: Digital radiography: A comparison with modern conventional imaging. *Postgrad Med J* 2006;82(969):425-428.
20. Polikeit A, Ferguson SJ, Nolte LP, Orr TE: The importance of the endplate for interbody cages in the lumbar spine. *Eur Spine J* 2003;12(6):556-561.
21. Polikeit A, Ferguson SJ, Nolte LP, Orr TE: Factors influencing stresses in the lumbar spine after the insertion of intervertebral cages: Finite element analysis. *Eur Spine J* 2003;12(4):413-420.
22. Fengbin Y, Jinhao M, Xinyuan L, Xinwei W, Yu C, Deyu C: Evaluation of a new type of titanium mesh cage versus the traditional titanium mesh cage for single-level, anterior cervical corpectomy and fusion. *Eur Spine J* 2013;22(12):2891-2896.
23. Lowe TG, Hashim S, Wilson LA, et al: A biomechanical study of regional endplate strength and cage morphology as it relates to structural interbody support. *Spine (Phila Pa 1976)* 2004;29(21):2389-2394.
24. Barsa P, Suchomel P: Factors affecting sagittal malalignment due to cage subsidence in stand-alone cage assisted anterior cervical fusion. *Eur Spine J* 2007;16(9):1395-1400.
25. Lim TH, Kwon H, Jeon CH, et al: Effect of endplate conditions and bone mineral density on the compressive strength of the graft-endplate interface in anterior cervical spine fusion. *Spine (Phila Pa 1976)* 2001;26(8):951-956.
26. Chiang MF, Teng JM, Huang CH, et al: Finite element analysis of cage subsidence in cervical interbody fusion. *J Med Biol Eng* 2004;24(4):201-208.
27. Adam C, Pearcy M, McCombe P: Stress analysis of interbody fusion—finite element modelling of intervertebral implant and vertebral body. *Clin Biomech (Bristol, Avon)* 2003;18(4):265-272.